POLITECNICO
MILANO 1863

SCUOLA DI INGEGNERIA INDUSTRIALE
E DELL'INFORMAZIONE

Executive Summary of the Thesis

GNSS anti-jamming techniques based on Controlled Radiation Pattern Antenna

Laurea Magistrale in Telecomunication Engineering - Ingegneria Delle Telecomunicazioni

Author: Lorenzo Danelli

Advisor: Prof. Lorenzo Luini

Co-advisor: Dr. Livio Marradi, Eng. Niccolò Pastori, Ph.D. Andrea Emmanuele

Academic year: 2021-2022

1. Introduction

The Global Navigation Satellite System (GNSS) covers a fundamental role for our society, providing Position Velocity and Time (PVT) information in several fields of application. The GNSS services are put in danger by jamming and spoofing attacks, wanted or unwanted signals able to disrupt or to inhibit the right GNSS signal reception. The Controlled Radiation Pattern Antenna (CRPA) are sophisticated receiving systems (stand-alone antenna or antenna plus receiver) which take advantage of an antenna array and linearly combining the signals received by the single antenna elements obtain a dynamically controlled array radiation pattern capable of reacting to interference attacks. In this scenario, Thales Alenia Space Italia (TAS-I), an European space sector leader, is active in the research on CRPA systems as interference-resistant GNSS equipment. This summary is the product of the work carried out in the frame of two TAS-I projects: Ground Reference Station Work Order 1 (GRS WO1), a GNSS reference station, and GAlileo Multi-purpose and Multi-frequency Antenna (GAMMA), a GNSS user receiver antenna. Both the systems are designed to guarantee robustness against jamming attacks. The main focus is set on techniques for jammers number estimation, null-steering methods and Direction Of Arrival (DOA) estimation implemented in the project GAMMA. The performance of the algorithms are investigated through MATLAB simulations that consider the peculiarities of the project GRS WO1 as study case. The best candidate algorithms, that meet the proper design specification of GAMMA, are here theoretically described. Finally, the results of the test campaign carried out on Array Receiver Board (ARB) and on the fully integrated GAMMA antenna, are reported in details and they verify the results obtained during the project simulation phase.

2. Signal model

Considering an array of N elements. It is possible to label $\vec{r_n}(x, y, z)$ the position of each $n = 1, ..., N$ array element in the space. Considering M transmitted signals $s_m(t)$ generated from different far-field sources at frequency f_m, as a function of time t. Each signal impinges on the array with a specific DOA, that can be labelled as $\alpha_m(\theta_m, \phi_m)$. Figure 1 represents a

scheme of the environment geometry description. The steering vector $a(\alpha_m)$, it is defined as $[1, e^{jkr\vec{2}\cdot\vec{u_m}}, ..., e^{jkr\vec{N}\cdot\vec{u_m}}]^T$ with dimension $N \times 1$ and it identifies a specific DOA of the signal.

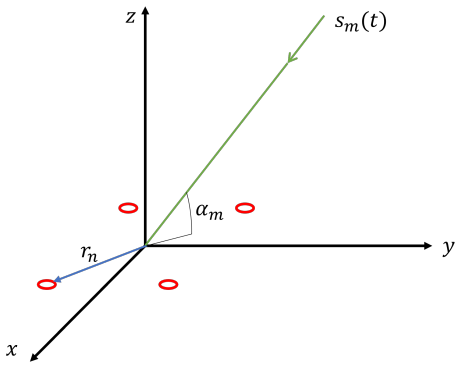

Figure 1: Environment geometry description in case of $N = 4$ antennas represented in red, $M = 1$ impinging signal in green.

The sampling frequency is labelled as f_{samp}. It is possible to define the number of samples as $N_{samp} = T_{obs} \cdot f_{samp}$. The transmitted signal can be represented as $X = [x_1, x_2, ...x_M]^T$ of dimensions $M \times N_{samp}$ where each row is x_m the sampled signal s_m. The same for the received signal $Y = [y_1, y_2, ...y_N]^T$ of dimensions $N \times N_{samp}$ where each row is y_n, the sampled signal of s_n, for which it holds:

$$Y = A \cdot X + N \tag{1}$$

where $A = [a(\alpha_1), a(\alpha_2), ..., a(\alpha_M)]$ is called Manifold matrix and has a dimensions $N \times M$ where the columns are constituted by the steering vectors of all the transmitted signals, N is the matrix of the sampled complex additive noise introduced by the receiver chains of dimension $N \times N_{samp}$. The sample covariance matrix R_y of the sampled received signal is written as:

$$R_y = \frac{1}{N_{samp}} Y \cdot Y^H \tag{2}$$

it has a dimension $N \times N$. Its eigenvalues and the eigenvectors are respectively labelled as λ_i and u_i. The eigenvectors are orthogonal and describe the space of the received signal. It is possible to rewrite (2) in the following way:

$$R_y = \sum_{i=1}^{N} \lambda_i \cdot u_i u_i^H \tag{3}$$

Moreover, if the signals are independent, the spectral decomposition of the matrix leads to identifying two different orthogonal subspaces: the signal plus noise subspace and the only noise subspace [1]. The following equation rewrites (3) to underline the existence of the two subspaces just introduced:

$$R_y = U_s \Lambda_s U_s^H + U_n \Lambda_n U_n^H \tag{4}$$

where $U_s = [u_1, ..., u_M]$ is a $N \times M$ dimension matrix, $\Lambda_s = diag(\lambda_1, ..., \lambda_M)$ is a $M \times M$ dimension matrix, $U_n = [u_{M+1}, ..., u_N]$ is a $N \times (N - M)$ dimension matrix, $\Lambda_n = diag(\lambda_{M+1}, ..., \lambda_N)$ is a $(N - M) \times (N - M)$ dimension matrix.

3. Controlled Radiation Pattern Antenna

The CRPA acts as a spatial filter capable to place a null or a beam, i.e. a specific direction of the space in which the gain array pattern is reduced or increased. Despite, the increment in the number of antennas implicates an increment in the complexity of the receiver, cost of material and power consumption.

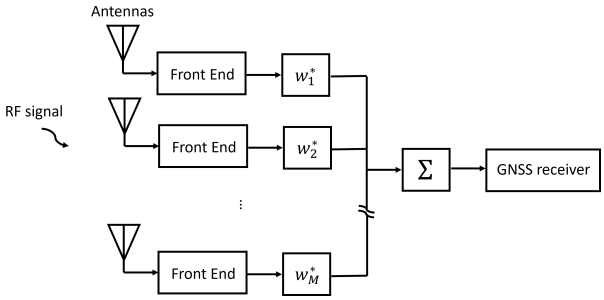

Figure 2: CRPA antenna scheme

Figure 2 shows a scheme of a CRPA where it is possible to understand the increased complexity of the receiver. In particular, each chain is multiplied by a complex factor w_i^*, called weight because it determines the contribution of the chain in the linear combination. It is important to underline that the weights computed must be conjugate before the application. In general, the array radiation pattern describes the amplitude and phase responses that the array introduces in each direction of the space $f_{ar}(\theta, \phi)$ and it is given by:

$$f_{ar}(\theta, \phi) = \sum_{n=1}^{N} w_n^* \cdot f_{el,n}(\theta, \phi) \tag{5}$$

where $f_{el,n}$ is the n-th antenna elements radiation response.

4. Jammers number estimation

The Maximum-Minimum Eigenvalue (MME) [2] and the Eigenvalue Ratio (ER) methods exploit the eigenvalues λ of the covariance matrix of the received signals R_y. From preliminary simulations, the MME method reveals to be reliable only in ideal case, i.e. considering the receiver chains perfectly balanced. Instead, ER method is discarded from the GAMMA design because it can not reach the reliability level ensured by the Power Spectrum Density (PSD) of the sampled received signal. This method turned out to be the best candidate for the number of jammers algorithm, it has been implemented in tha GAMMA ARB and it is exposed in the detail in the following subsection.

4.1. Jammers number estimation from PSD of the signal

The PSD of the received signal ($\frac{V}{Hz}$ or $\frac{dBW}{Hz}$) is compared with a certain Threshold (THR) to identify the presence of jammers. The Power Spectrum Density (PSD) of the signal is:

$$PSD(f_k) = \frac{1}{N_k \cdot f_s} \left| \sum_k Y \cdot e^{-j2pifkT_c} \right|^2 \quad (6)$$

where f_k is the sampled frequency, $N_k = T_{obs} \cdot f_s$ is the number of samples considered in the Discrete Fourier Trasform (DFT) that is given by the product of sampling frequency f_s and the observation time T_{obs}. The argument of the module is the DFT of the sampled signal that could be also implemented as a Fast Fourier Trasform (FFT). The THR is evaluated in case of only noise reception, by multiplying the highest PSD value measured in a certain time interval (e.g of 10 seconds) $PSD_{noise,max}$ by a constant k, so:

$$THR = k \cdot PSD_{noise,max} \quad (7)$$

The number of blocks of PSD samples over the THR is equal to the estimated number of jammers M_{est}. One disadvantage of this method is that it can not distinguish two different jammers with overlapped bandwidth since it would mix them up detecting only one jammer and generating an under-estimation case.

5. Null-steering weights

The null-steering algorithm has the purpose to compute the weights vector w that generates an equivalent antenna gain pattern with nulls in direction of the interfering signals. The Minimum Variance Distortionless Response (MVDR) [1] and the Power Inversion (PI) methods [3] exploit the covariance matrix R_y of the received signals. However, they are discarded because their simulation results, in terms of interference rejections, are not compliant with the performance required. The MUltiple SIgnal Classification (MUSIC) null-steering method is a subspace method that is described in the following subchapter. In particular, one-eigenvector MUSIC is a specific case that has the peculiarity to be independent from the number of jammers estimation. Otherwise, the MUSIC-MVDR and the MUSIC-PI methods are hybrid techniques that mixes the characteristic of the algorithms previously described. They have really good performance, comparable to the subspace methods, but they are dependent on the number of jammers estimation.

5.1. MUSIC null-steering

The MUSIC algorithm is a subspace method since it exploits the eigenstructure decomposition of the spatial covariance matrix R_y, shown in (4). The eigenvectors corresponding to the M_{est} highest eigenvalues compose the signal subspace U_s while the others the noise subspace U_n. Moreover, U_s spans the same subspace as the Manifold matrix A. So, any steering vector that belongs to the Manifold matrix subspace verifies the following equation:

$$U_n^H a(\theta, \phi) = 0 \quad (8)$$

that is why a linear combination of the steering vector of the signal as $a(\alpha)$, in this case, is orthogonal to the noise space U_n:

$$w_{MUSIC} = U_n \cdot c_{vect} \quad (9)$$

where U_n is the noise subspace matrix of dimension $N \times (N - M_{est})$ composed by the eigenvectors of the noise and c_{vect} is a coefficient vector of dimension $(N - M_{est}) \times 1$. When $c_{vect} = [0, ..., 0, 1]$ the weights vector is equal to the eigenvector linked to the smallest eigenvalue $w_{MUSIC} = u_N$, removing the problem of the number of jammers estimation dependency.

6. DOA estimation

The DOA estimation algorithms are based on the so-called power spectrum $P(\theta, \phi)$ that is a spatial estimator with polar angle coordinates dependency. The Conventional and the MVDR specta exploit the sample covariance matrix R_y. They are methods extremely unreliable in case of more than one jammers due to their limited spatial resolution. On the other hand, the MUSIC spectrum is the best method and it is exposed in the detail in the following subsection.

6.1. MUSIC spectrum

The MUSIC spectrum is based on the subspace decomposition of the only noise subspace U_n. It is possible to exploit the orthogonality of the only noise subspace U_n and the signal steering vector $a_n(\theta, \phi)$, in particular with equation (8), to create the MUSIC spectrum:

$$P_{MUSIC}(\theta, \phi) = \frac{1}{a(\theta, \phi)^H U_n U_n^H a(\theta, \phi)} \quad (10)$$

Indeed, the denominator of MUSIC spectrum tends to zero when the steering vector points at the jammer DOA, in this way, the overall spectrum increases creating a peak. This algorithm is highly dependent on the the jammers number estimation M_{est} to correctly operate the subspace division and to know the number of spectrum peaks to search. An important aspect, that must be taken into account when adopting a subspace method, is the correct sizing of the noise and signal subspaces. Indeed, an over sizing of the noise subspace has detrimental impact on the DOA estimation removing a signal peak from the spectrum. While the under-sizing of the noise subspace is less impacting.

7. Hardware in the loop tests

This chapter presents the hardware test performed on the GAMMA ARB in TAS-I laboratory. The GAMMA ARB, shown in Figure 3, is in charge of computing the null-steering weights, the frequency, the DOA and JRN of the interference signal. The ARB presents four Radio Frequency (RF) signal inputs to collect the signals from the four antenna elements. Two operational frequency bands are designed: a low band from $1164\,MHz$ to $1300\,MHz$ and a higher band from $1559\,MHz$ to $1591\,MHz$.

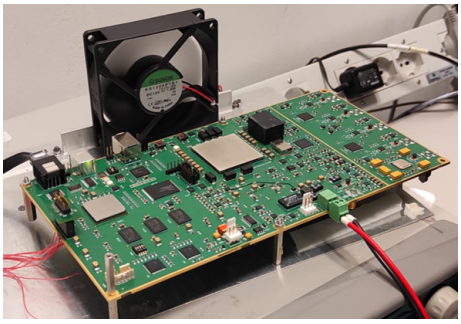

Figure 3: Array Receiver Board of GAMMA

In particular, GAMMA implements a static calibration of the 4 RF chains and a static computation of the two THRs for the number of jammers estimation (for high and low bands), operated before each test. The calibration acts directly on the unbalanced covariance matrix of the received signal R'_y in order to obtain the calibrated one $R'_{y,c}$. A typical jammer power (6 dB over the GNSS signal power) is assumed.
Figure 4 shows a scheme of setup used, composed by a signal generator connected with a RF cable to a CRPA emulator that, in turn, is connected with four short RF cables to the ARB. The CRPA emulator is digitally commanded and capable of emulating the different phase shifts and attenuations of the received signal introduced by the multiple radiating elements of the antenna. The calibration of this setup is performed imposing, to each chain of the CRPA emulator, $0dB$ of attenuation and $0deg$ of phase delay.

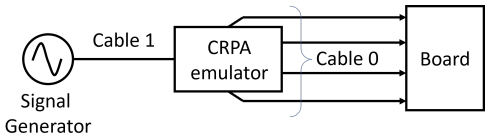

Figure 4: Single jammer multiple DOA setup

7.1. Miss-detection error and false alarm

Figure 4 shows the setup arranged to compute the percentages of miss-detection and false alarms in case of a single jammer with CW or AWGN $1MHz$ band modulation or only noise. No miss-detections is observed during the tests while a very limited percentage of false alarm (lower than $0,2\%$) is experimented. In particular, an over-estimation error of one jammer is

performed each time that the signal generator changes the frequency of the signal. Indeed, during the jammer frequencies transition, the ARB experiments an integration time in which the PSD detects two jammer frequencies. Therefore, in this specific integration time, the number of estimated jammers is two. Despite this errors, no false alarm is generated in only noise condition, showing that the calibration of the THRs for the number of jammers estimation is very robust.
Moreover, using two signal generators connected to a combiner, it is possible to exploit the same setup to perform detection tests with two simulated jammers. In particular, two cases are tested: two jammers in the same receiver band (but not overlapped in frequency) and in different bands. The percentage of false alarm errors in the tests is zero while the miss-detection one is about 1%. The errors of miss-detection occur contextually with the changes of the signal frequency. Indeed, the detection of three interferences, out from the GAMMA project goals, causes the ARB CPU usage overload.

7.2. Null-steering jammer rejection and DOA error

Figure 4 shows the setup arranged to evaluate the jammer rejection achieved with the null-steered antenna pattern and the error of the DOA estimation. A CW modulated signal, centred in a frequency range included in GAMMA high band is generated. For each signal frequency, the CRPA emulator imposes attenuations and a phase delays on the four channels that emulate the reception of a signal with the following DOAs $[0, 90]deg$, $[-60, 70]deg$, $[134, 50]deg$, $[120, 30]deg$ and $[0, 10]deg$, (Azimuth, Elevation).
Exploiting the Equation (5), it is possible to obtain in post-processing the null-steered antenna pattern rejections in the emulated DOAs with the element weights computed by the ARB. Figure 5 shows the mean of the array gain pattern rejections in the emulated jammer DOAs experimented during the test. The stability of the jammer rejection in time is stable considering each single emulated DOA. The minimum guaranteed jammer rejection, introduced by the null-steered gain pattern, is -12dB while the highest one is -35dB. The different rejection capability w.r.t. the jammer DOA is likely due to the azimuthal array geometry. Indeed, the highest rejection is achieved when the Azimuth of the jammer is centred between one element and the next one (inter-element), while the lowest rejection is obtained one when the Azimuth exactly matches an antenna element.

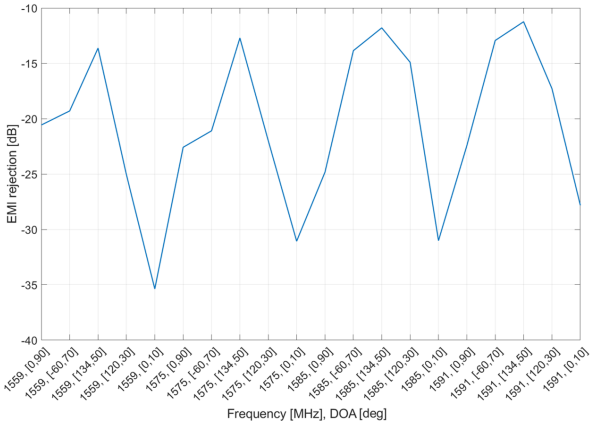

Figure 5: Post-processing EMI rejection of the array pattern with MUSIC weights from ARB.

Figure 6 shows DOA estimation error, computed as Root Mean Square Error between the error committed on Azimuth and Elevation domains, of the data collected during the test. The maximum experimented DOA error is $4,5deg$. This Hardware in the loop test result confirms the simulation one fulfilling the requirements. It is possible to notice an higher DOA error at low elevation angle.

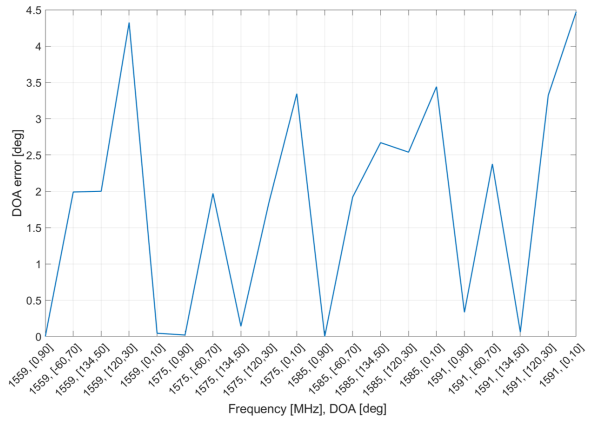

Figure 6: DOA estimation error from ARB.

Figures 7 show an example of the MUSIC spectra obtained post-processing the calibrated covariance matrix $R'_{y,c}$ and the uncalibrated one R'_y, related to the same integration period. This MUSIC spectra comparison proves the uncon-

ditioned need of the calibration process for the DOA estimation algorithm to work correctly.

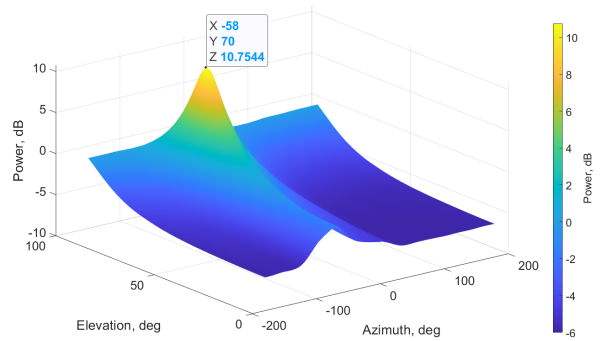

(a) Calibrated

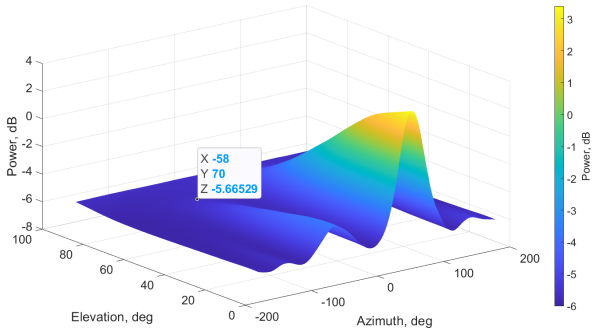

(b) Uncalibrated

Figure 7: Calibrated and uncalibrated MUSIC power spectra: number of jammers $M = 1$, emulated DOA $[-60, 70]\,deg$

8. Conclusions

The number of jammers estimation from PSD reveals to be very reliable in case of wideband receiver and fixed narrowband jammers. On the other hand, the PSD methods can occur in miss-detection error, when the jammer scenario foresees two signals with the same frequency or wide band jammer, and in false alarm, when a fast frequency-variant jammer is present. The alternative number of jammers estimation algorithm, ER, can overcome all of these vulnerabilities. Although, other weaknesses have to be taken into account as the dependency on the quality of the calibration, the limited maximum number of detectionable jammers and a detrimental effect brought by the chain unbalancing.
Regarding null-steering algorithms, the subspace methods derived from MUSIC proved higher performance w.r.t the PI and MVDR methods. The one-eigenvector MUSIC and the MUSIC-PI do not need any antenna pattern measurement, obtaining therefore an independence from measurement errors and a cost reduction. Moreover, the one-eigenvector MUSIC loses any dependency from the estimated number of jammers and grants optimum performance in term of jammer rejection.
Preliminary analysis on conventional and MVDR spectra, revealed their unreliability in case of more than one jammers. Indeed, only the MUSIC spectrum has been considered and investigated in detail. The high reliability of the jammers number estimation, showed in the tests, contributes to the good performance of the DOA estimation algorithm correctly dividing the noise and signal subspaces.
The hardware tests on the GAMMA ARB show performance of the selected algorithms in line with the results obtained during the project simulation phase.

9. Acknowledgements

I would like to thank Prof. Lorenzo Luini, Dr. Livio Marradi, Eng. Niccolò Patori and Ph.D. Andrea Emmanuele not only for the incredible opportunity received and all knowledge shared about the GNSS and CRPA, without which this work could not exist, but also for the availability and the passion shown. I acknowledge also all the TAS-I navigation technology group that helps and integrates me creating a constructive working atmosphere.

References

[1] P.-J. Chung, M. Viberg, and J. Yu. DOA Estimation Methods and Algorithms. In *Academic Press Library in Signal Processing*, volume 3, pages 599–650. Elsevier, 2014.

[2] M. Hamid, N. Bjorsell, and S. Ben Slimane. Sample covariance matrix eigenvalues based blind SNR estimation. In *2014 IEEE International Instrumentation and Measurement Technology ConferenceProceedings.*

[3] G. Carrie, F. Vincent, T. Deloues, D. Pietin, and A. Renard. A New Blind Adaptive Antenna Array for GNSS Interference Cancellation. In *Conference Record of the Thirty-Ninth Asilomar Conference onSignals, Systems and Computers, 2005.*, pages 1326–1330.